Epitaxial growth of titanium oxycarbide on MgO (0 0 1) substrates by pulsed laser deposition

Hien Do[*], Tzu-Chun Yen, Chih-Sheng Tian, Yue-Han Wu, Li Chang

Department of Materials Science and Engineering, National Chiao Tung University, Hsinchu, 1001, Tahsueh Road, Taiwan, ROC

ABSTRACT

Epitaxial TiC_xO_y thin films were grown on MgO (0 0 1) substrates by using pulsed laser deposition method. High-resolution X-ray diffraction and transmission electron microscopy were used to examine crystallinity and microstructure of epitaxial TiC_xO_y film on MgO. The chemical composition of the film is determined to be $x \sim 0.47$ and $y \sim 0.69$ by X-ray photoelectron spectroscopy. Atomic force microscopy revealed that the surface of TiC_xO_y film is very smooth with roughness of 0.18 nm. The resistivity of the TiC_xO_y film measured by four-point-probe method was about 137 $\mu\,\Omega$ cm.

© 2010 Elsevier B.V. All rights reserved.

1. Introduction

Titanium carbide (TiC) has become a very attractive material due to its unique mechanical and physical properties such as high hardness and high strength, good stability at high temperatures, excellent electrical and thermal conductivity, low coefficient of friction, and high corrosion and oxidation resistance [1]. These properties make TiC strong candidates in many applications including cutting tools, wear coatings, passive layers, catalysis, and high temperature electronic devices [1–4]. In terms of chemical bonding, TiC is found to exist not only in the stoichiometric form, but also in the substoichiometric and overstoichiometric form [5–9], in which TiC can have up to a maximum of 50% or even more vacancies in the carbon sublattice and still retain its NaCl crystal structure [10]. Based on these properties, TiC promises to be a great candidate for multifunctional applications by adding the third element to the Ti–C matrix. It has been shown that the addition of nitrogen to TiC films can reduce the inner stress, electrical resistivity, and friction coefficients [11,12]. The addition of oxygen to the Ti–C films, especially in the substoichiometric ones, was also found to be of great interest due to its high reactivity with most of the metals and the possibility of tailoring the optical and mechanical properties between those of metallic-like carbides and those of the corresponding ionic oxides by varying the oxygen/carbon ratio [13,14]. Therefore, titanium oxycarbide (TiC_xO_y) has been considered as a thin film coating material for decorative and electronic applications [13–15].

Most of titanium oxycarbide films have been grown by chemical vapor deposition (CVD) and magnetron sputtering on various substrates such as Si, glasses, high speed-steels, and stainless steels [13,14,16–19]. However, in order to obtain high-quality TiC_xO_y films, those methods require a relatively high substrate temperature which may lead to serious problems for many applications. Pulsed laser deposition (PLD) which has been widely used over the past decade is an attractive alternative for the deposition of high-quality thin films because of its unique advantages as described in the following [20,21]. With the energetic laser-target interaction, PLD is particularly capable of deposition of hard materials such as TiC, TiN, and TiC_xO_y that are difficult to synthesize in bulk and by other deposition methods. However, there have been no previous reports of epitaxial growth of TiC_xO_y films, in comparison with those of TiC and TiN growth which has been extensively studied.

In this paper, we report the successful growth of epitaxial titanium oxycarbide films on MgO (0 0 1) substrates using pulsed laser deposition. The reason that MgO is chosen as substrate is based on consideration of the same crystal structure (rock-salt) and small lattice mismatch between them. The crystallinity, microstructure, chemical composition, morphology of titanium oxycarbide were investigated using X-ray diffraction (XRD), transmission electron microscopy (TEM), X-ray photoelectron spectroscopy (XPS), and atomic force microscopy (AFM), respectively. The resistivity of the films was determined by four-point-probe method.

2. Experimental

The deposition was carried out in a vacuum chamber with base pressure of 10^{-6} Torr. The KrF ($\lambda = 248$ nm) laser beam was

---

* Corresponding author. Tel.: +886 3 5731615; fax: +886 3 5724727.
  E-mail address: dohienvl@gmail.com (H. Do).

incident at an angle of 45° with respect to a 2-in. diameter oxygen-containing TiC target with composition of $TiC_1O_{0.5}$ determined by XPS. A 2-in. MgO (0 0 1) substrate was ultrasonically cleaned in acetone and ethanol, dried with nitrogen gas, and immediately loaded into the vacuum chamber. The substrate was faced the target at a distance of 140 mm. The target was rotated to avoid pitting during deposition. Prior to TiC_xO_y growth, MgO (0 0 1) substrate was heat-treated at 700 °C for 30 min to obtain a clean and smooth surface. The growth process was then carried out under the condition of a laser pulse repetition rate of 5 Hz, substrate temperature at 700 °C, and laser power density of 2–3 J/cm². TiC_xO_y films were grown in Ar gas ambient of 10^{-4} Torr. After 2 h of deposition time, the growth process was completed. The deposited films were characterized by XRD using a Bede D1 high-resolution X-ray diffractometer equipped a two-bounce Si 220 channel-cut collimator crystal, a dual channel Si 220 analyser crystal (DCA), and Cu $K\alpha_1$ radiation ($\lambda = 1.5406$ Å). X-ray photoelectron spectroscopy (ULVAC-PHI, PHI quantera SXM) was used to determine chemical composition of TiC_xO_y using an Al $K\alpha$ radiation source. For XPS quantitative analysis, relative sensitivity factors from manufacture's program and database were used. Cross-sectional TEM specimens were prepared by tripod polishing method, followed by Ar-ion milling at angle of 4–6° and acceleration voltage of 4–4.5 kV. TEM observations were then carried out in a JEOL 2010F microscope. The surface morphology of the deposited films on MgO (0 0 1) was examined with AFM (D3100). A four-point-probe was used to measure the resistivity of the deposited films.

3. Results and discussion

X-ray diffraction pattern of a titanium oxycarbide film is shown in Fig. 1a. It is seen only (0 0 2) and (0 0 4) reflections of TiC_xO_y and MgO, suggesting a textured or epitaxial relationship between the deposited film and MgO substrate. The d-spacing of (0 0 2) is determined to be 2.146 Å. As shown in Fig. 1b of the X-ray rocking curve measurement of (0 0 2) TiC_xO_y, the full width at half maximum (FWHM) is 133 arcsec, indicating that TiC_xO_y grown on MgO has a very good quality. The X-ray φ-scan was also performed, using {0 2 2} reflections of substrate and film, to verify the epitaxy between the deposited film and MgO substrate. As shown in Fig. 2, four {0 2 2} diffraction peaks separated by 90° appear at the same φ angles for both the film and the substrate. This result illustrates that the deposited film has epitaxially grown on MgO with the cube-on-cube relationship of TiC_xO_y(0 0 1)//MgO(0 0 1) and TiC_xO_y[1 0 0]//MgO[1 0 0]. Fig. 3 shows the X-ray reflectivity curve of the TiC_xO_y film deposited on MgO, from which the film thickness can be determined to be 45 nm. As a result, the growth rate is estimated to be approximately 22.5 nm/h.

The state of strain of the deposited TiC_xO_y film was investigated by using XRD reciprocal space map (RSM) of asymmetric (1 1 3) MgO and (1 1 3) TiC_xO_y reflections. The vertical (Q_y) and horizontal (Q_x) axes shown in Fig. 4 lie along MgO [0 0 1] and MgO [1 1 0] directions, respectively. Both MgO and TiC_xO_y reflections are almost vertically aligned, showing that TiC_xO_y has strong coherency with MgO. The corresponding out-of-plane, c, and in-plane, a, lattice parameters can be determined by $c = 3/Q_y$, and $a = \sqrt{2}/Q_x$ [22,23]. Using MgO (1 1 3) peak as reference with known lattice parameter ($a = 4.211$ Å), the lattice parameters of TiC_xO_y can be $c = 4.289$Å and $a = 4.228$Å. The difference between in-plane and out-of-plane lattice parameters ($c/a = 1.0144$) suggests that the TiC_xO_y film is compressively strained with a tetragonal distortion resulting from the small lattice mismatch of TiC_xO_y with MgO. Based on the above data and using the Poisson coefficient of TiC ($\nu = 0.17$), the cubic lattice parameter of TiC_xO_y can be determined approximately to be about 4.237Å.
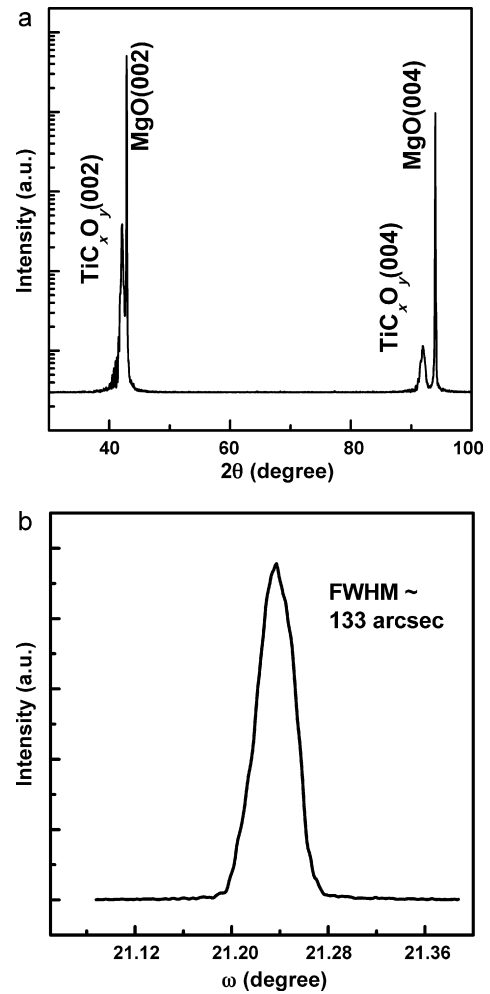
Fig. 1. XRD (a) 2θ–θ scan and (b) ω-scan for TiC_xO_y film deposited on MgO (0 0 1).

Chemical composition of the TiC_xO_y film was determined by XPS measurements. Fig. 5 shows high-resolution C-1s, Ti-2p, and O-1s XPS spectra for TiC_xO_y as a function of the Ar sputtering time. As shown in Fig. 5a, the C-1s spectrum from the deposited TiC_xO_y surface after air exposure shows that there are three components. The peak at 284.9 eV is assigned to hydrocarbon contamination [24].
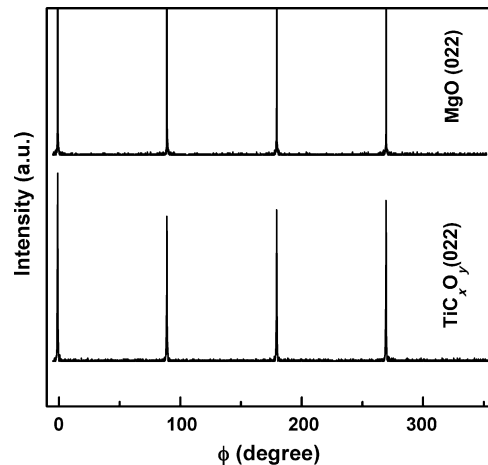
Fig. 2. XRD φ-scan of {0 2 2} planes for TiC_xO_y film on MgO (0 0 1) substrate, showing that epitaxial relationship between the film and the substrate is TiC_xO_y(0 0 1)//MgO(0 0 1) and TiC_xO_y [1 0 0]//MgO[1 0 0].
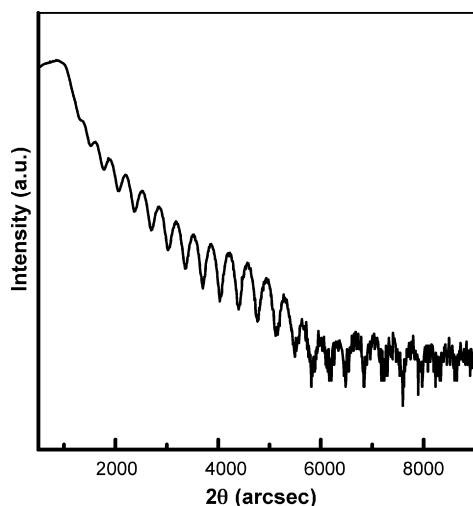
Fig. 3. X-ray reflectivity curve for the deposited TiC$_x$O$_y$ film.

Fig. 4. Reciprocal space map of the asymmetric (1 1 3) for TiC$_x$O$_y$ film on MgO.

The peak with lower energy at 281.8 eV corresponds to Ti–C bond [25,26]. The weak peak observed at 288.8 eV is typical for C–O bond. After 1 min of surface cleaning by Ar sputtering, only one C-1s peak corresponding to Ti–C bond is observed. Similar situation is also found for Ti-2p signal (Fig. 5b). The spectrum of Ti-2p before surface cleaning exhibits two groups of Ti-2p$_{3/2}$ and Ti-2p$_{1/2}$. In addition of Ti–C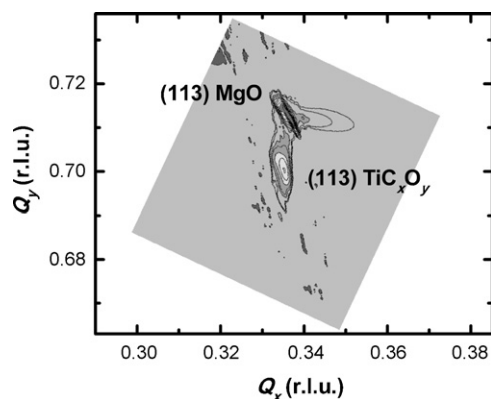 bonds at 454.9 and 460.8 eV, the Ti-2p$_{3/2}$ component at 458.4 eV corresponds to Ti–O bond in TiO$_2$, and it disappeared after only 1 min of Ar sputtering. Instead, only Ti-2p$_{3/2}$ component at 454.9 eV can be observed [25,26]. This component also contains Ti-2p$_{3/2}$ in TiO that has been reported to have a peak value at 455.1 eV [27]. The O-1s XPS spectrum (Fig. 5c) of the air-exposed TiC$_x$O$_y$ film exhibits a broad peak that can be decomposed into two components at 530 eV and 531.5 eV. The peak at 530 eV corresponds to O-1s in TiO$_2$ [28]. The higher binding energy peak at 531.5 eV can be assigned to O-1s in TiO [24,29]. After 1 min of Ar sputtering, only a single peak at 531.5 eV is observed. The XPS depth profile in Fig. 5d shows that the film has a uniform chemical composition.
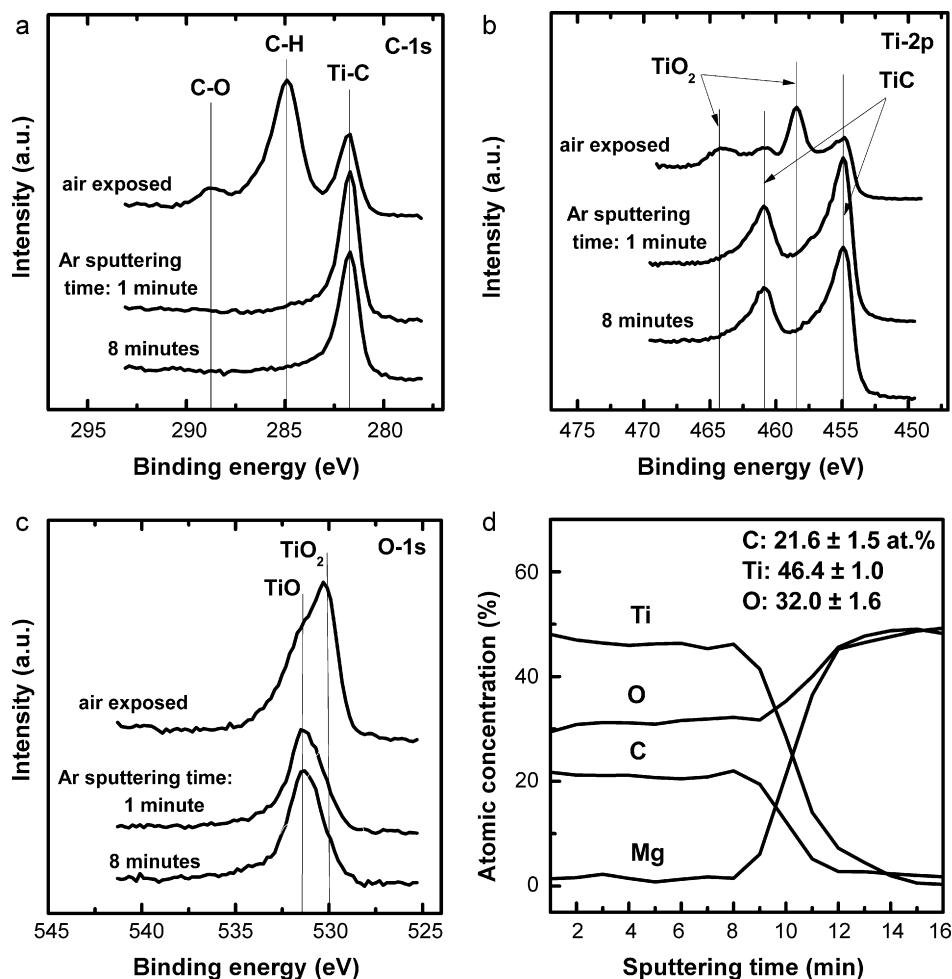

Fig. 5. XPS spectra for (a) C-1s, (b) Ti-2p, (c) O-1s, as a function of Ar sputtering time, and (d) XPS depth profile for TiC$_x$O$_y$ film deposited on MgO.
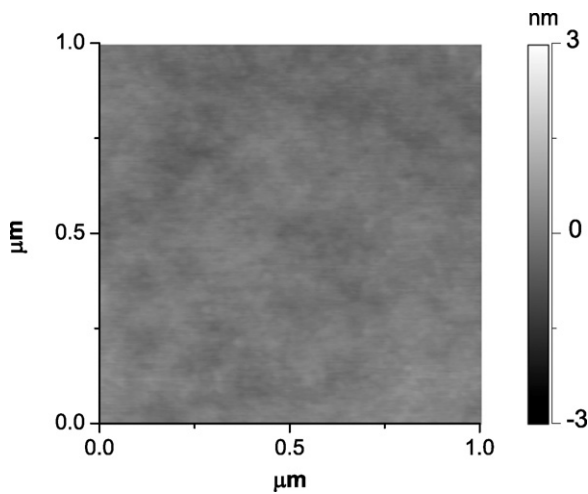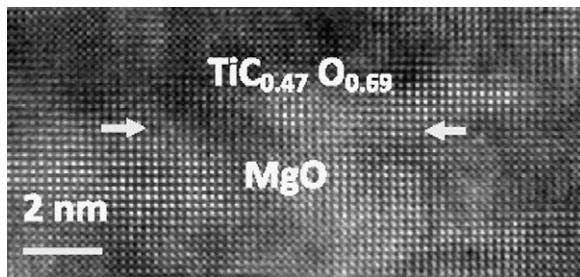
Fig. 6. AFM image of $TiC_{0.47}O_{0.69}$ film surface.

Fig. 7. Cross-sectional HRTEM image along [1 0 0] zone axis showing a sharp interface between $TiC_{0.47}O_{0.69}$ and MgO. No misfit dislocations are observed at the interface over the range of 15 nm.

The average chemical composition can be determined from the values from 1 to 8 min of sputtering time and shown in the insert of Fig. 5d. As a result, the stoichiometry of titanium oxycarbide is about $TiC_{0.47}O_{0.69}$. According to the data available in literature about the relationship between lattice parameter and stoichiometric coefficients x and y of TiC_xO_y, the lattice parameter is in the range of 4.246–4.280 Å [30,31] in good agreement with the value determined from our XRD data as described above. The higher oxygen content in the deposited film compared with that of target can be considered as a consequence of residue of oxygen in the reaction chamber that might contribute 9–22 at.% to the composition of TiC films grown even under high vacuum (1.5×10^{-7} Torr) [26]. This residual oxygen could strongly react with Ti ions emitted from laser ablation plume [32] due to high affinity between them. Also it is often found oxygen incorporation in deposited TiN films by PLD due to the interaction of Ti ions with oxygen [33,34].

The surface morphology of the $TiC_{0.47}O_{0.69}$ film on MgO (0 0 1) was examined by AFM. As can be seen in Fig. 6, the film surface is very uniform and smooth with root-mean-square (RMS) roughness about 0.18 nm.

Cross-sectional high-resolution TEM analysis was performed to confirm the epitaxial growth of $TiC_{0.47}O_{0.69}$ on MgO. Fig. 7 shows a sharp interface without any interlayer between $TiC_{0.47}O_{0.69}$ and MgO. As can be seen clearly in Fig. 7, no misfit dislocations generated at the interface can be identified across the observation range of 15 nm, supporting that the in-plane lattice mismatch between $TiC_{0.47}O_{0.69}$ and MgO is very small in consistence with the XRD results.

The resistivity of the $TiC_{0.47}O_{0.69}$ film as measured by four-point-probe method is about 137 $\mu\,\Omega$ cm that lies in the resistivity range between bulk TiC (55 $\mu\,\Omega$ cm) [35] and bulk TiO (190 $\mu\,\Omega$ cm) [36].

This value is smaller than that of epitaxial $TiC_{0.8}$ films that has been reported to be 200 $\mu\,\Omega$ cm [37]. The high oxygen content in the TiC_xO_y film is considered to be responsible for the high resistivity of TiC_xO_y compared with that of pure TiC. It is analogous with the case of epitaxial TiN_x films. The resistivity of oxygen-containing epitaxial TiN_x films increases with oxygen concentration and can be in the range from 21.0 to 32.3 $\mu\,\Omega$ cm that is larger than that of the oxygen-free epitaxial TiN_x ($\sim$15 $\mu\,\Omega$ cm) [34]. The $TiC_{0.47}O_{0.69}$ film deposited in our case is specially much more electrically conducting compared with polycrystalline TiC_xO_y and TiN_xO_y films that have shown the resistivity in the order of magnitude of mΩ cm [13,38].

4. Conclusions

It has been demonstrated that high-quality epitaxial TiC_xO_y films can be deposited on MgO (0 0 1) substrates by pulsed laser deposition at 700 °C. XRD and TEM show that the epitaxial relationship between the film and the substrate is TiC_xO_y (0 0 1)//MgO(0 0 1) and TiC_xO_y [1 0 0]//MgO[1 0 0]. The film composition as determined by XPS is $TiC_{0.47}O_{0.69}$. The deposited $TiC_{0.47}O_{0.69}$ film has a smooth surface with roughness of 0.18 nm, and is electrically conducting with resistivity of 137 $\mu\,\Omega$ cm. The tetragonal distortion of the deposited film determined from RSM measurement illustrates that the 45 nm thick film is under compressive strain.

References

[1] H.O. Pierson, Handbook of Refractory Carbides and Nitrides: Properties, Characteristics, in: Processing and Applications, Noyes Publication, Westwood, New Jersey, USA, 1996.
[2] S.T. Oyama, Catal. Today 15 (1992) 179.
[3] J.D. Parsons, G.B. Kruaval, A.K. Chaddha, Appl. Phys. Lett. 65 (1994) 2075.
[4] A.K. Chaddha, J.D. Parsons, G.B. Kruaval, Appl. Phys. Lett. 66 (1995) 760.
[5] K.E. Tan, A.M. Bratkovsky, R.M. Harris, A.P. Horsfield, D. Nguyen-Manh, D.G. Pettifor, A.P. Sutton, Modelling Simul. Mater. Sci. Eng. 5 (1997) 187.
[6] A. Mani, P. Aubert, F. Mercier, H. Khodja, C. Berthier, P. Houdy, Surf. Coat. Technol. 194 (2005) 190.
[7] S. Jhi, S.G. Louie, M.L. Cohen, J. Ihm, Phys. Rev. Lett. 86 (2001) 15.
[8] A. Czyzniewski, W. Precht, J. Mater. Process. Technol. 157–158 (2004) 274.
[9] W. Prencht, A. Czyzniewski, Surf. Coat. Technol. 174–175 (2003) 979.
[10] W. Williams, Int. J. Refract. Met. Hard Mater. 17 (1999) 21.
[11] H. Dimigen, C.P. Klages, Surf. Coat. Technol. 49 (1991) 543.
[12] D. Monaghan, D. Teer, P. Logan, I. Efeoglu, R. Arnell, Surf. Coat. Technol. 60 (1993) 525.
[13] A.C. Fernandes, P. Carvalho, F. Vaz, S. Lanceros-Mendez, A.V. Machado, N.M.G. Parreira, J.F. Pierson, N. Martin, Thin Solid Films 515 (2006) 866.
[14] L. Marques, H. Pinto, A.C. Fernandes, O. Banach, M.M.D. Ramos, F. Vaz, Appl. Surf. Sci. 255 (2009) 5615.
[15] D. Munteanu, R. Cozma, B. Borcea, F. Vaz, J. Opt. Adv. Mater. 8 (2006) 712.
[16] G. Georgiev, N. Feschiev, D. Popov, Z. Uzuuov, Vacuum 36 (1986) 595.
[17] J.F. Sundgren, B.O. Johansson, S.E. Karlsson, Thin Solid Films 105 (1983) 353.
[18] A.C. Fernandes, P. Carvalho, F. Vaz, N.M.G. Parreira, Ph. Goudeau, E. Le Bourhis, J.P. Rivière, Plasma Process. Polym. 4 (2007) S83–S88.
[19] A.C. Fernandes, L. Cunha, C. Moura, F. Vaz, P. Carvalho, E. Le Bourhis, Ph. Goudeau, J.P. Rivière, N.M.G. Parreira, Surf. Coat. Technol. 202 (2007) 946.
[20] D.B. Chrisey, G.K. Hubler (Eds.), Pulsed Laser Deposition of Thin Films, Wiley, New York, 1994.
[21] M.A. El Khakani, M. Chaker, M.E. O'Hern, W.C. Oliver, J. Appl. Phys. 82 (1997) 4310.
[22] R.J. Kennedy, P.A. Stampe, J. Cryst. Growth 207 (1999) 200.
[23] C.H. Chen, A. Saiki, N. Wakiya, K. Shinozaki, N. Mizutani, J. Cryst. Growth 219 (2000) 253.
[24] R. Sanjinsés, H. Tang, H. Berger, F. Gozzo, G. Margaritondo, F. Lévy, J. Appl. Phys. 75 (1994) 2945.
[25] H. Ihara, Y. Kumashiro, A. Itoh, K. Meada, Jpn. J. Appl. Phys. 12 (1973) 1462.
[26] O. Rist, P.T. Murray, Mater. Lett. 10 (1991) 323.
[27] D. Simon, C. Perrin, J. Bardolle, J. Microsc. Spectrosc. Electron. 1 (1976) 175.
[28] H.K. Jang, S.W. Whangbo, Y.K. Choi, Y.D. Chung, K. Jeong, C.N. Whang, J. Vac. Sci. Technol., A 18 (2000) 2932.
[29] J. Yao, J. Shao, H. He, Z. Fan, Vacuum 81 (2007) 1023.

[30] A. Afir, M. Achour, N. Saoula, J. Alloys Compd. 288 (1999) 124.
[31] I.L. Shabalin, V.M. Vishnyakov, D.J. Bull, S.G. Keens, L.F. Yamshchikov, L.I. Shabalin, J. Alloys Compd. 472 (2009) 373.
[32] L. D'Alessio, A. Galasso, A. Santagata, R. Teghil, A.R. Villani, P. Villani, M. Zaccagnino, Appl. Surf. Sci. 208–209 (2003) 113.
[33] N. Biunno, J. Narayan, S.K. Hofmeister, A.R. Srivatsa, R.K. Singh, Appl. Phys. Lett. 54 (1989) 1519.
[34] R. Chowdhury, R.D. Vispute, K. Jagannadham, J. Narayan, J. Mater. Res. 11 (1996) 1458.
[35] P Ettymayer, W Lengauer, in: R.B. King (Ed.), Carbides: Transition Metal Solid State Chemistry, vol. 2, Wiley, Chichester, 1994, pp. 519–531.
[36] C.N.R. Rao, W.E. Wahnsiedler, J.M. Honig, Solid State Chem. 2 (1970) 315.
[37] L. Norin, S. McGinnis, U. Jansson, J.-O. Carlsson, J. Vac. Sci. Technol., A 15 (1997) 3082.
[38] Mu-Hsuan Chan, Fu-Hsing Lu, Surf. Coat. Technol. 203 (2008) 614.